ChemComm

Size and shape evolution of core–shell nanocrystals

C. J. Zhong,* W. X. Zhang, F. L. Leibowitz and H. H. Eichelberger

Department of Chemistry, State University of New York at Binghamton, Binghamton, New York 13902, USA. E-mail: cjzhong@binghamton.edu

Received (in Columbia, MO, USA) 20th April 1999, Accepted 19th May 1999

The findings of an investigation of temperature-manipulated size and shape evolution for pre-formed decanethiolate–encapsulated gold nanocrystals are described.

Monolayer-encapsulated metal nanoparticles are of considerable technological interest because of the potential electronic, optical, magnetic, catalytic and sensing applications emerging from the core–shell combinations.[1,2] Part of our motivation stems from the opportunities of manipulating such structural properties as interfacial building blocks towards fine-tunable electrode nanomaterials.[3] One important advance emerging from various synthetic strategies[4–16] is the two-phase method, which was first reported by Schiffrin and coworkers[4,5] and has been extensively utilized.[1,4–8] This relatively simple method, which involves transferring an aqueous tetrachloroaurate ($AuCl_4^-$) precursor into an organic phase followed by reduction in the presence of thiols (RSH), has been proven very effective for synthesizing core sizes ranging from 1.5 to 5 nm by controlling the RSH/Au ratio and reaction temperature.[4–8] Narrow-size preparation and shape control are the ultimate synthetic challenges. Relatively little is, however, known about shape control for such composite nanomaterials,[12–16] though examples have recently been demonstrated for platinum nanoparticles by manipulating precursor ratios,[14] or introducing 'shape-inducing reagent'.[15] In view of the molecular and crystal natures of such core–shell systems, size and shape are inherently a dynamic process and an evolution may occur as a result of changes in chemical potentials of the particles. Such a process is the basis of crystallography involving nucleation, dissolution and growth,[18,19] but to our knowledge has not been studied for the core–shell type systems. Here, we describe the preliminary results of an investigation of such a process of pre-formed thiolate-encapsulated gold nanoparticles by manipulating temperatures.

Thiolate-encapsulated gold nanoparticles were prepared first by the two-phase method.[4,6] Briefly for decanethiolate-encapsulated nanoparticles, after transferring an aqueous $AuCl_4^-$ by tetraoctylammonium bromide (98%) into a toluene phase, decanethiol (DT, 96%) was added at a 2:1 ratio of DT/Au, and followed by adding an excess (12 ×) of an aqueous reducing agent ($NaBH_4$, 99%). The reaction produced a dark-brown solution of the DT-encapsulated nanoparticles, which was then subjected to two types of sample handling procedures. In the first procedure, the solvent was removed by rotary evaporator (at *ca.* 50 °C) yielding a black and waxy product, DT/Au(**1**). In the second procedure, the solution was brought to *ca.* 110 °C under reduced pressure for *ca.* 30 min. Upon this treatment, the solution showed a color change from brownish to pinkish. We note here two observations for the heating treatment. First, simply heating the solution at temperatures between 50 and 110 °C did not lead to any color change. Secondly, a color change occurred under conditions of the concentration rising to *ca.* 10-fold and the temperature to 100–115 °C. A systematic study of the related factors is in progress. This treatment was performed after the formation of the encapsulated nanoparticles, a procedure different from temperature control during the synthesis.[8] After removing solvent, the gray and powdery product, DT/Au(**2**), was collected. Both **1** and **2** were subjected to subsequent cycles of suspension in ethanol and acetone and centrifugation for at least four times to ensure a complete removal of non-nanoparticle materials.

These two samples, DT/Au(**1**) and DT/Au(**2**), were first examined by transmission electron microscopy (TEM). Fig. 1 presents two representative TEM images from the two samples. For the DT/Au(**1**) sample [Fig. 1(*a*)], the result displays an average core size of *ca.* 2.0 nm with *ca.* 80% populations within the range 1.5–2.5 nm. The crystal shapes, though not clearly identifiable with the TEM resolution, appear non-uniform. These microscopic features are in good agreement with those reported previously for samples prepared under similar conditions.[8] A previous study has determined that the most likely shape for such a core size is a truncated octahedron.[12] In contrast to the results shown for the DT/Au(**1**) sample, two striking features are evident for the DT/Au(**2**) sample [Fig. 1(*b*)]. First, it displays an increased core size with a narrow distribution in which more than 90% populations are within the range 4.7–5.7 nm (average 5.2 nm). Second, a close examination of the particle shapes indicates a 'hexagon' outline for an observable percentage of the particles. Clearly, an evolution in both size and shape of the particles has occurred from DT/Au(**1**) to DT/Au(**2**) samples. While not reported for thiolate-encapsulated nanocrystals, temperature-induced changes in size and morphology, including quasimelting, coalescence and sintering of fine particles, have indeed been reported for metal or metal oxide crystals or nanocrystals.[18,19] The size and shape evolution of our encapsulated nanoparticles in the solution may involve a

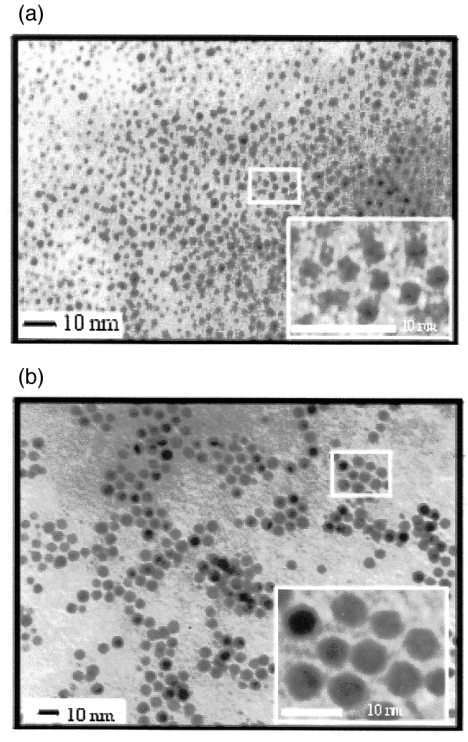

Fig. 1 TEM micrographs of two DT-encapsulated Au nanocrystal samples: (a) DT/Au(**1**) and (b) DT/Au(**2**) on carbon-coated TEM grids. The insert represents an enlarged view of the indicated area.

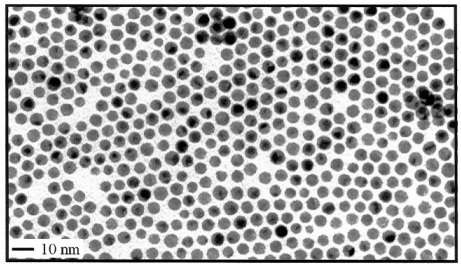

Fig. 2 TEM micrograph of the ordered domain features for DT/Au(**2**) on a carbon-coated TEM grid.

balance of the chemical potentials *via* desorption and re-adsorption of the shell components and coalescence of the cores as the driving force for the eventual size and shape.

Another remarkable feature for the evolved nanocrystals was the formation of long range order upon casting a solution of the DT/Au(**2**) sample onto a TEM grid and evaporating the solvent. As shown in Fig. 2, large domains of long range self-organizations are evident. Two-dimensional ordered arrays with a hexagon-type arrangement can also be identified. Similar long range orders have recently been reported for alkanethiolate-encapsulated gold nanoparticles that were prepared without temperature treatment, for examples, by fractionalized dodecanethiolate-encapsulated gold particles,[12] by gas-phase synthesis followed by solution-phase encapsulation,[10] and most recently by two-phase synthesized gold particles coated with quaternary ammonium ion pairs.[5] Our observation serves as an intriguing example for the long range ordering for the encapsulated nanocrystals prepared by the temperature treatment. In an excellent agreement with the notion that the encapsulating chains are likely interdigitated between opposing alkyl shells,[1,5,10,12] the determined average core–core (edge-to-edge) distance of *ca.* 1.5 nm is indeed close to the expected chain length of DT (1.4–1.5 nm).

Two sets of spectroscopic data further confirmed the observed evolution and the associated structural properties. First, the optical properties for the samples before and after the size and shape evolution were determined by measurement of adsorption in the visible region. Optically, fine particles display surface plasmon resonance bands with intensity and energy strongly dependent on size. The UV-VIS spectrum for DT/Au(**1**) in hexane displays an identifiable surface plasmon band envelope around 510 nm. The shape and position of this band is in agreement with those previously reported for similar particle sizes.[8] In contrast, the spectrum for the DT/Au(**2**) sample exhibits an increased intensity for the 520 nm band. This result, without an apparent shift in energy, is consistent with an increase in core size, a well documented phenomenon.[6,8,12]

Secondly, the structural properties of the encapsulating monolayer shells were characterized using IR spectroscopy. Two pieces of evidence emerge from the spectral similarities and differences (Fig. 3) between these two samples. First, the overall similarity in both high and low energy regions suggests the absence of major structural changes such as decomposition and transformation. Second, a close examination of the C–H stretching region provides diagnostic information about ordering properties of the alkyl chains in the shell. While bands corresponding to methyl stretching (2955 and 2872 cm^{-1}) show little change, a shift to lower wavenumbers is identified for the asymmetric and symmetric methylene stretching bands from DT/Au(**1**) (2920 and 2950 cm^{-1}) to DT/Au(**2**) (2917 and 2948 cm^{-1}). As extensively studied for both monolayers on planar[17] and on nanocrystal gold,[6,8] such a shift is diagnostic of the more crystalline nature[25] of the monolayer on larger particles. These results, combined with the optical data, confirm the evolution of the smaller-sized to larger-sized nanocrystals with the integrity of the final encapsulating shell structures maintained.

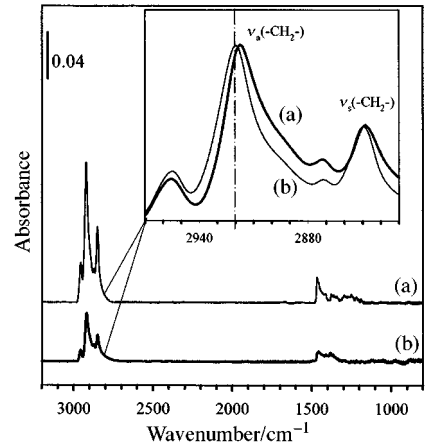

Fig. 3 FTIR spectra for (a) DT/Au(**2**) and (b) DT/Au(**1**) samples in KBr pallets. The insert represents a normalized view in the C–H stretching region.

Finally, we note that similar microscopic and spectroscopic characteristics have also been observed for samples with alkanethiolate shell components of different chain lengths.

A further systematic investigation to unravel the mechanistic aspects is in progress.

Notes and references

1 M. J. Hostetler and R. J. Murray, *Curr. Opin. Colloid Interface Sci.*, 1997, **2**, 42 and references therein.
2 G. Schon and U. Simon, *Colloid Polym. Sci.*, 1995, **273**, 101; 1995, **273**, 202.
3 C. J. Zhong, W. X. Zheng and F. L. Leibowitz, *Electrochem. Commun.*, 1999, **1**, 72.
4 M. Brust, M. Walker, D. Bethell, D. J. Schiffrin and R. Whyman, *J. Chem. Soc., Chem. Commun.*, 1994, 801.
5 J. Fink, C. J. Kiely, D. Bethell and D. J. Schiffrin, *Chem. Mater.*, 1998, **10**, 922.
6 M. J. Hostetler, J. J. Stokes and R. W. Murray, *Langmuir*, 1996, **12**, 3604.
7 M. J. Hostetler, C. J. Zhong, B. K. H. Yen, J. Anderegg, S. M. Gross, N. D. Evans, M. D. Porter and R. W. Murray, *J. Am. Chem. Soc.*, 1998, **120**, 9396.
8 M. J. Hostetler, J. E. Wingate, C. J. Zhong, J. E. Harris, R. W. Vachet, M. R. Clark, J. D. Londono, S. J. Green, J. J. Stokes, G. D. Wignall, G. L. Glish, M. D. Porter, N. D. Evans and R. W. Murray, *Langmuir*, 1998, **14**, 17.
9 R. G. Freeman, K. C. Garbar, K. J. Allison, R. M. Bright, J. A. Davis, A. P. Guthrie, M. B. Hommer, M. A. Jackson, P. C. Smith, D. G. Walter and M. J. Natan, *Science*, 1995, **267**, 17.
10 R. P. Andres, J. D. Bielefeld, J. I. Henderson, D. B. Janes, V. R. Kolagunta, C. P. Kubiak, W. J. Mahoney and R. G. Osifchin, *Science*, 1996, **273**, 1690.
11 R. Elghanian, J. J. Storhoff, R. C. Mucic, R. L. Letsinger and C. A. Mirkin, *Science*, 1997, **277**, 1078.
12 R. L. Whetten, J. T. Khoury, M. M. Alvarez, S. Murthy, I. Vezmar, Z. L. Wang, P. W. Stephens, C. L. Cleveland, W. D. Luedtke and U. Landman, *Adv. Mater.*, 1996, **8**, 428.
13 Z. L. Wang, J. M. Petroski, T. C. Green and M. A. El-Sayed, *J. Phys. Chem. B*, 1998, **102**, 6145.
14 T. S. Ahmadi, Z. L. T. C. Wang, T. C. Green, A. Henglein and M. A. El-Sayed, *Science*, 1996, **272**, 1924.
15 Y.-Y. Yu, S.-S. Chang, C.-L. Lee and C. R. C. Wang, *J. Phys. Chem. B*, 1997, **101**, 6661.
16 M. Giersig and P. Mulvaney, *Langmuir*, 1993, **9**, 3408.
17 M. D. Porter, T. B. Bright, D. L. Allara and C. E. Chidsey, *J. Am. Chem. Soc.*, 1987, **109**, 3559.
18 M. Miki-Yoshida, S. Tehuacanero and M. Jose-Yacaman, *Surf. Sci.*, 1992, **274**, 569.
19 S. Lijima and P. M. Ajayan, *J. Appl. Phys.*, 1991, **70**, 5138.

Communication 9/03165K